On small scale vortices in turbulent flows

By J. Jiménez

It has been known for a long time that the small scales of turbulent flows are not completely random. It was first shown by Batchelor & Townsend (1949) that the statistics of the velocity derivatives are incompatible with an uncorrelated random behavior of the velocity field at scales comparable to the Kolmogorov dissipation limit. In particular, the n-th order flatness factors of the velocity derivatives would be universal constants for a gaussian random velocity field, whereas experiments show them to be functions of the Reynolds number. The original experiments were extended and refined several times, both in the laboratory (Kuo & Corrsin, 1971, Champagne, 1978) and in numerical simulations (Siggia & Patterson, 1978), with generally consistent results. A summary of the available data can be found in (Van Atta & Antonia, 1980).

It was soon realized that these results implied the existence of intermittent organized structures at the short wavelength end of the spectrum, and experiments were attempted to clarify their geometry . It was Kuo & Corrsin (1972) who first presented suggestive evidence that the high vorticity loci were vortex tubes or, at most, ribbons, but it was necessary to wait for the advent of direct visualizations of numerically simulated flows before these more or less flattened vortex tubes were shown to be the dominant structures of isotropic turbulent flows at high vorticity amplitudes (Siggia, 1981, Kerr, 1985, Hosokawa & Yamamoto, 1990, She *et al.*, 1990, Ruesch & Maxey, 1991, Vincent & Meneguzzi, 1991). A re-examination of older data fields in numerically simulated turbulent shear layers, homogenous shear flows, and channels shows the presence of compact vortices of roughly similar characteristics. These will be discussed below. Finally (Douady *et al.*, 1991) produced direct experimental visualizations of strong concentrated persistent vortices in homogeneous turbulence, and (Schwarz, 1990) published pictures of organized strain structures which show up as alternating bands of consistent orientation of flakes suspended in a grid-stirred flow. It is not clear how or whether these structures are connected to the vortex tubes, but they are persistent and seem to have comparable dimensions.

We will summarize here the experimental evidence available for these compact, small scale vorticity structures, using both published results and other available numerical flow fields. That evidence will be discussed in the next section and shows that there is a certain homogeneity of the small structures across flows whose large scale character is very different. We will then use those general characteristics to define a simple model for the small scale vortices and, in particular, to explain some of the experimental observed relations between the vorticity and the rate of strain tensor. Our main result is that many of those properties turns out to be essentially kinematic.

Phenomenology

The definition of a vortex tube is a subjective matter that probably varies among different authors, but it seems to refer in most cases to the structures with the highest values of vorticity in the flow (although some adjustment has to be done in wall bounded flows for the presence of very strong vortex layers at the wall). It may be possible, however, to get some idea of their characteristic sizes and strengths by comparing data from different sources.

There seems to be reasonable agreement that the diameter of the tubes is intermediate between the Taylor microscale, λ, and the Kolmogorov scale, η, in the range of $4-10\eta$. However, since most estimates come from numerical simulations for which $Re_\lambda \simeq 100$ and $\lambda/\eta \simeq 15$, it is difficult to distinguish between low multiples of η and high fractions of λ. The vortex length is quoted as being of the order of either a small multiple of λ or of the integral scale of the flow, L. Again, since $L/\lambda \simeq Re_\lambda^{1/2}/5 \simeq 2$, for $Re_\lambda \approx 100$, it is difficult to distinguish both possibilities.

Still harder to estimate is the intensity of the vortices, which can usually be derived only indirectly from other quantities given by the different authors. It is expressed best as a Reynolds number based on the total circulation, γ, in the tube

$$Re_\gamma = \gamma/\nu.$$

It is interesting that whenever this quantity can be estimated, it seems to be in the range, $Re_\gamma \sim 100-500$ (see Table 1 and Appendix I for the derivation of the different cases). This is true even for flows like the wall region in a channel or like the turbulent mixing layer, in which the detailed turbulence dynamics are presumably quite different from those of homogeneous turbulence. Once more, since all the observations come from numerical simulations at low Reynolds numbers and given the uncertainties in the calculation of the circulation, it is difficult to know whether the information in Table 1 should be interpreted as a range for Re_γ or as evidence for a dependence on Re_λ. From the analysis of the only two cases in which data are available for several Reynolds numbers - the channel and the homogeneous shear flow (see Appendix I) - there is some reason to believe that the circulation of the cores is an increasing function of the bulk Reynolds number, at least in the range for which experimental data are available.

On the other hand, $Re_\gamma \simeq 150$ is at least a plausible value for the intensity of the smallest observable vortices. Since the vortices are defined as loci of very high vorticity, they have to be produced by stretching of previous structures, which is the only mechanism able to amplify vorticity away from walls but which does not modify the total circulation. As long as a vortex is being stretched, there is no limit as to how thin its core can become, and there is a well known equilibrium solution (Burger's vortex, see Batchelor, 1967), for which the rate of strain, S, compensates viscous dissipation at a radius of order $(S/\nu)^{1/2}$. The structures in which we are interested, though, are supposed to survive longer than their own inertial time scale, even after the strain that originated them ceases to act. Otherwise, they could not be considered more coherent that the background motion, and their dynamical

Flow type	γ/ν	ω_{max}/ω'	ρ/η	$\Delta u/u'$	
Homog. isotropic turb.	260	8.9	3.1	3.5	$Re_\lambda = 60$
Wall region of channel	100-300	4.6	4.3	3.9	$Re_\tau = 100 - 200$
Homogeneous shear	400-500	5.6	5.3	3.0	$Re_\lambda = 95$
Plane mixing layer	340	20.	2.5	6.7	$Re_\lambda = 55$

TABLE 1. Characteristic circulation associated to small scale vortices in various types of flows. See Appendix I for detailed references and assumptions.

significance would be small. In fact, all the available observations indicate that their lifetime is long.

It can easily be shown that the peak vorticity of a two dimensional axisymmetric, unstrained, self similar vortex, diffusing under the effect of viscosity, decays by a factor of two in a time

$$\tau = \frac{Re_\gamma T_E}{16\pi^2}, \tag{1}$$

where $T_E = 4\pi^2\rho^2/\gamma$ is the turnover time at the $1/e$ radius, ρ, or the core . Because of the large denominator in (1), vortices with Re_γ much smaller than 150 decay too fast and would not be identified as coherent.

It is interesting that in all the cases that we have studied, the radius of the cores, normalized with $\eta = (\omega'/\nu)^{1/2}$, is of the order of 3-4. This is roughly the radius of an equilibrium Burgers' vortex under a rate of strain $O(\omega')$, which can be expected to be the average fluctuating rate of strain within the flow. While the estimation of individual radii is subject to large uncertainties, the relative consistency of the values in Table 1 makes it likely that the thickness of the cores is really the Kolmogorov scale and that they are Burgers' vortices. Note that as noted in Appendix I, the large radii for the homogeneous shear flow is probably related to numerical resolution effects.

In all the cases that we have studied, the peak vorticity at the axis of the cores is several times higher than the r.m.s. vorticity for the flow field (Table 1). The same is true for the characteristic velocity, $\Delta u = \omega_{max}\rho$, compared to the r.m.s. velocity fluctuation for the flow considered as a whole. This means that the flow in the immediate neighborhood of the vortices is dominated by them and is relatively independent of the influence of other structures. We will show now that this can be used to understand some of the alignment properties that have been reported in recent years between the different velocity derivatives.

Alignment

It was first suggested by Kerr (1985) and shown later by Ashurst *et al.* (1987a) that the vorticity in homogeneous turbulent flows is preferentially aligned with the eigenvector corresponding to the intermediate eigenvalue of the rate of strain tensor, $S_{ij} = (\partial_j u_i + \partial_i u_j)/2$, especially at high values of the enstrophy. This was confirmed

later in other flows, both in numerical simulations (Vincent & Meneguzzi, 1990) and in laboratory experiments (Dracos *et al.*, 1989). That observation was considered surprising because the lagrangian vorticity equation can be written as

$$d\omega_i/dt = S_{ij}\omega_j + \nu\nabla^2\omega_i$$

and it had always been assumed that the vorticity vector would be stretched along the direction of any eigenvector of the rate of strain tensor with a positive eigenvalue and that it would eventually be aligned to the eigenvector of the most positive one. In fact, the existence of tubes was also considered initially controversial because it can be shown that the most probable state for the rate of strain tensor is to have two extensional eigenvalues (Betchov, 1956), and it was felt that this should give rise preferentially to vortex sheets.

That this is not necessarily so can be seen by considering *two dimensional* vortices and vortex sheets. In those cases, the vorticity is normal to the $x-y$ plane and generates a rate of strain tensor in which the only two non-zero eigenvalues are equal in magnitude and opposite in sign, with eigenvectors normal to the vorticity. Thus the vorticity is aligned with the eigenvector of the intermediate (zero) eigenvalue and is not stretched by any of the other two. Since the picture that emerges from the previous survey of experimental results, at least at high enstrophy values, is one of elongated, essentially two dimensional, compact vortices, it is not surprising that the rate of strain produced by them is normal to their axes and that it dominates the rate of strain tensor, so that any residual eigenvector is, by the orthogonality property, aligned to the vorticity. It is only the residual axial eigenvalue that does the stretching or compression of the vortex tube, while the two equatorial ones are just local effects of the vorticity and do not participate in its dynamics. Note that this arrangement automatically satisfies the requirement that two eigenvalues of the rate of strain tensor be positive, while being consistent with the observation of a prevalence of tubes.

This interpretation is reinforced by Figure 1, which is adapted from (Ashurst *et al.*, 1987b) and which shows that the pressure gradient, conditioned on the angle which it forms with each of the three eigenvectors, is maximum when it is aligned to the intermediate one and 45^0 away from either the most compressive or extensive eigenvector. It is easy to recognize in this arrangement the strain generated around a two dimensional vortex, in which the pressure gradient is directed away from its axis, while the two principal strains are normal to it and aligned 45^0 away from the radial direction (Note that the interpretation of this figure in the original reference is different from the one given here).

In a turbulent field, Figure 2 shows a section of a compact core taken normal to its vorticity. The field corresponds to the head of a hairpin vortex in the simulation of a homogeneous turbulent shear flow in (Rogers & Moin, 1987), which was one of the flows used by (Ashurst *et al.*, 1987ab). The figure also shows the eigenvectors corresponding to the most compressive and to the most extensive eigenvalues, projected on the plane of the section. It is clear that while outside the vortex the orientations of the vectors are irregular, inside it they correspond essentially to that of a simple plane shear.

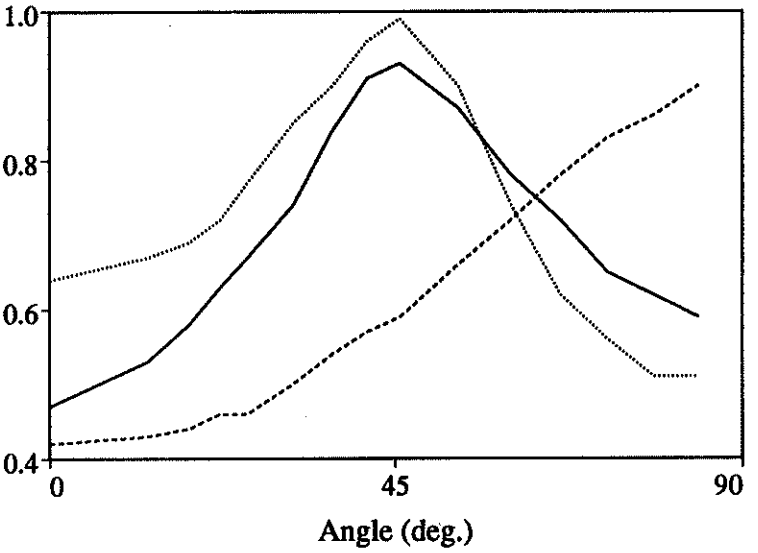

FIGURE 1. Averaged squared pressure gradients in a turbulent field, measured along lines forming a given angle to each principal strain axis. Solid line: Angle measured to most extensional eigenvector. Dotted: Most compressive. Dashed: Intermediate. Adapted from (Ashurst *et al.*, 1987b).

The argument can be made a little more general. Consider a vorticity distribution, $\mathbf{\Omega}(\mathbf{x})$, which in some neighborhood can be written as

$$\mathbf{\Omega}(\mathbf{x}) = \omega_0(\mathbf{x})\,\mathbf{v_3} + \mathrm{O}(\omega'), \tag{2}$$

where bold-faced quantities are three dimensional vectors, $\mathbf{v_3}$ is the unit vector along the x_3 axis, and $\omega_0 \gg \omega'$. Assume moreover that $\partial\omega_0/\partial x_1$ and $\partial\omega_0/\partial x_2$ are $\mathrm{O}(\omega_0)$, but note that the solenoidal character of the vorticity implies that $\partial\omega_0/\partial x_3 = \mathrm{O}(\omega')$. We can express the velocity, $\mathbf{u}$, in general as

$$\mathbf{u}(\mathbf{x}) = -\frac{1}{4\pi}\int \frac{(\mathbf{x}-\mathbf{x}')\times\mathbf{\Omega}(\mathbf{x}')}{|\mathbf{x}-\mathbf{x}'|^3}\,\mathrm{d}^3\mathbf{x}', \tag{3}$$

plus a potential part which is independent of the vorticity and which will be assumed to be $\mathrm{O}(\omega')$. Differentiating with respect to x_i, and integrating by parts we obtain the velocity gradient as

$$\partial u_j/\partial x_i = -\frac{1}{4\pi}\int \frac{1}{|\mathbf{x}-\mathbf{x}'|^3}\,[(\mathbf{x}-\mathbf{x}')\times\partial\mathbf{\Omega}/\partial x_i']_j\,\mathrm{d}^3\mathbf{x}', \tag{4}$$

plus small terms coming from the potential. It can be seen after some reflection that the part of this deformation tensor that is $\mathrm{O}(\omega_0)$ is confined to the top 2×2 diagonal submatrix. Under those conditions, the generic eigenvalue structure of the rate of strain tensor is formed by two dominant eigenvalues, $\mathrm{O}(\omega_0)$, whose eigenvectors

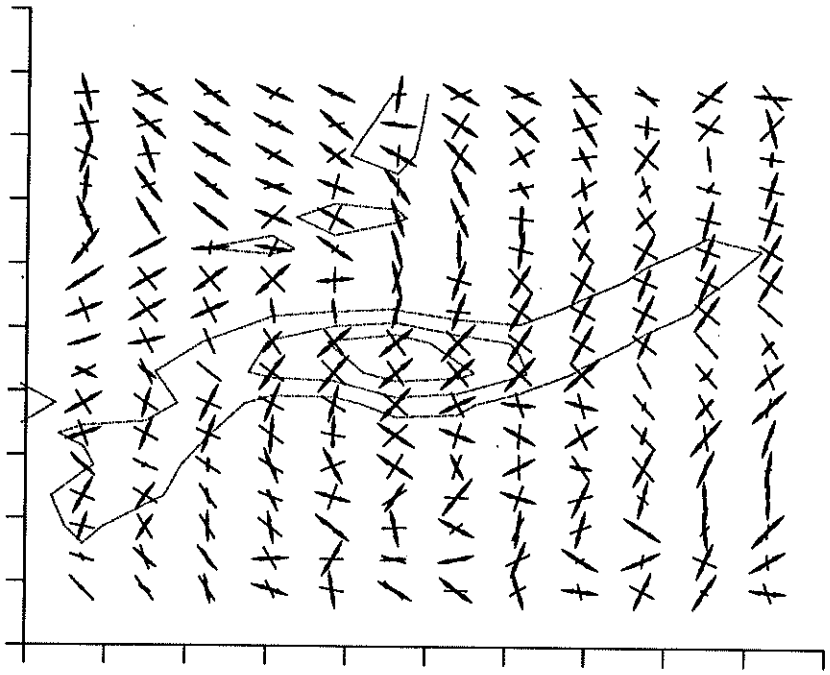

FIGURE 2. Section normal to a strong vortex core in the turbulent field in (Rogers & Moin, 1987). Dotted lines are isovorticity contours. Heavy arrowed lines are most extensional eigenvectors, projected in the plane of the figure. Light lines, without arrows, are most compressive eigenvectors. Eigenvectors are not scaled with eigenvalues. Length variation is due solely to projection.

form at most a small angle $O(\omega'/\omega_0)$ with the equatorial plane (x_1, x_2), and by a third eigenvalue, $O(\omega')$, whose eigenvector is similarly aligned to $\mathbf{v_3}$, and to the dominant vorticity. The strain structure discussed above for a two dimensional vortex is a particular case of this arrangement, but the argument is more general and should apply to other situations. It is important to realize that equations (3-4) are completely kinematic and that the alignment of the strains with respect to the vorticity is independent of the particular dynamical mechanism involved in the generation of the vorticity concentration (2).

In particular, it was suggested in (Kerr, 1985a, Ashurst *et al.*, 1987a), that the alignment of the vorticity to the intermediate eigenvector is due to the tendency of the vorticity vector to rotate in that direction as a consequence of the asymptotic behavior of the solutions of a truncated local approximation to the Navier Stokes equations (Vieillefosse, 1982). While those equations might still be useful in explaining the formation of the vorticity concentrations, the present discussion suggests that the explanation of the alignment is simpler and that it is the rate of strain tensor the one that rotates towards the vorticity once the latter becomes strong enough.

The same model can be used to explain some of the quantitative information

available on the magnitude of the strain eigenvalues at the points of maximum dissipation, which has been measured from numerical simulations to be approximately in the ratio (1:3:-4) (Ashurst *et al.*, 1987a). From the model that we have developed here, we may visualize those structures as stretched vortices in which the straining and the viscous diffusion are roughly in equilibrium. This would at least be true during the formation stage, at which dissipation is maximum. It is shown in Appendix II that the maximum rate of strain in those Burgers' vortices occurs in a annulus surrounding the core, slightly outside the $1/e$ vorticity radius. This distribution has been documented graphically in (Ruetsch & Maxey, 1991) for numerical isotropic turbulence. It is also shown in the appendix that at the point of maximum rate of strain, the ratio of the first two eigenvalues is $\sigma_2/\sigma_1 = 0.012Re_\gamma - 0.5$, which for $Re_\gamma \approx 200 - 400$, corresponding to the range of experimental values, varies between (1:2:-3) and (1:4:-5). These values are in rough agreement with the numerical ones quoted above, but they increase with vortex intensity. It would be interesting to check whether flows with a larger spread in the measured values of ω_{max}/ω' also have a larger value of the ratio of the principal strains, but the Reynolds numbers of the present numerical simulations are too low for that purpose.

Some of the data used for the phenomenological estimates were not contained in the original papers and have been made kindly available by Drs. Moser and Rogers for the purpose of this investigation. They also provided much of the data processing software. Their help is warmly appreciated.

REFERENCES

ASHURST, W. T., KERSTEIN, A. R., KERR, R. M. & GIBSON, C. H. 1987a Alignment of vorticity and scalar gradient with strain in simulated Navier Stokes turbulence. *Phys. Fluids.* **30**, 3243-3253.

ASHURST, W. T., CHEN, J. Y. & ROGERS, M. M. 1987b Pressure gradient alignment with strain rate and scalar gradient in simulated Navier Stokes turbulence. *Phys. Fluids.* **30**, 3293-3294.

BATCHELOR, G. K. 1967 *An introduction to fluid mechanics.* Cambridge Univ. Press, pp. 271-273.

BATCHELOR, G. K. & TOWNSEND, A. A. 1949 The nature of turbulent motion at large wave numbers. *Proc. Roy. Soc. London.* **A 199**, 238-255.

BETCHOV, R. 1956 An inequality concerning the production of vorticity in isotropic turbulence. *J. Fluid Mech.* **1**, 497-504.

CHAMPAGNE, F. H. 1978 The fine scale structure of the turbulent velocity field. *J. Fluid Mech.* **86**, 67-108.

DRACOS, T., KHOLMYANSKY, M., KIT, E. & TSINOBER, A. 1989 Some experimental results on velocity-velocity gradients measurements in turbulent grid flows. *Proc. IUTAM Symp. Topological Fluid Mech., Cambridge, August 13-18, 1989* (H.K. Moffat and A. Tsinober, eds.), Cambridge U. Press, pp. 564-584.

DOUADY, S., COUDER, Y. & BRACHET, M. E. 1991 Direct observation of the intermittency of intense vorticity filaments in turbulence. *Phys. Rev. Lett.* **67**, 983-986.

HOSOKAWA, I. & YAMAMOTO, K. 1990 Intermittency of dissipation in directly simulated fully developed turbulence. *J. Phys. Soc. Japan.* **59**, 401-404.

JIMÉNEZ, J. & MOIN. P. 1991 The minimal flow unit in near wall turbulence. *J. Fluid Mech.* **225**, 213-240.

KERR, R. M. 1985 Higher order derivative correlation and the alignment of small-scale structures in isotropic numerical turbulence. *J. Fluid Mech.* **153**, 31-58.

KIM, J., MOIN, P. & MOSER, R. 1987 Turbulence statistics in fully developed channel flow at low Reynolds number. *J. Fluid Mech.* **177**, 133-166.

KUO, A. Y. & CORRSIN, S. 1971 Experiments on internal intermittency and fine structure function in fully turbulent fluid. *J. Fluid Mech.* **50**, 285-319.

KUO, A. Y. & CORRSIN, S. 1972 Experiments on the geometry of the fine structure regions in fully turbulent fluid. *J. Fluid Mech.*. **56**, 447-479.

MOSER, R. D. & ROGER, M. M. 1991 Mixing transition and the cascade to small scales in a plane mixing layer. *Phys. Fluids.* **A 3**, 1128-1134.

ORLANDI, P. & JIMÉNEZ, J. 1991 A model for bursting of near wall vortical structures in boundary layers. *8th. Symp. Turb. Shear Flows, Munich, Sept. 9-11, 1991.*

ROBINSON, S. K. 1989 A review of vortex structures and associated coherent motions in turbulent boundary layers. *2nd IUTAM Symp. Structure of Turbulence and Drag Reduction, Zurich, July 25-28, 1989* (A. Gyr, ed.), pp. 22-50.

ROGERS, M. M. & MOIN, P. 1987 The structure of the vorticity field in homogeneous turbulent flows. *J. Fluid Mech.* **176**, 33-66.

RUETSCH, G. R. & MAXEY, M. R. 1991 Small scales features of vorticity and passive scalar fields in homogeneous isotropic turbulence. *Phys. Fluids.* **A 3**, 1587-1597.

SCHWARZ, K. W. 1990 Evidence for organized small scale structure in fully developed turbulence. *Phys. Rev. Lett.* **64**, 415-418.

SHE, Z.-S., JACKSON, E. & ORSZAG, S. A. 1990 Intermittent vortex structures in homogeneous isotropic turbulence. *Nature.* **344**, 226-228.

SIGGIA, E. D. 1981 Numerical study of small scale intermittency in three dimensional turbulence. *J. Fluid Mech.* **107**, 375-406.

SIGGIA, E. D. & PATTERSON, G. S. 1978 Intermittency effects in a numerical simulation of stationary three dimensional turbulence. *J. Fluid Mech.* **86**, 567-592.

TENNEKES, H. & LUMLEY, J. L. 1972 *A first course in turbulence*, MIT Press.

VAN ATTA, C. W. & ANTONIA, R. A. 1980 Reynolds number dependence of skewness and flatness factors of turbulent velocity derivatives. *Phys. Fluids.* **23**, 252-257.

VIEILLEFOSSE. P. 1982 Local interaction between vorticity and shear in a perfect incompressible fluid. *J. de Physique.* **43**, 837-842.

VINCENT, A. & MENEGUZZI, M. 1991 The spatial structure and statistical properties of homogeneous turbulence. *J. Fluid Mech.* **225**, 1-25.

WEI, T. & WILLMARTH, W. W. 1989 Reynolds-number effects on the structure of a turbulent channel flow. *J. Fluid Mech.* **204**, 57-95.

Appendix I: Data processing for vortex circulations.

To compute circulations we have assumed that the vorticity distribution inside the cores corresponds to that of a viscous axisymmetric vortex

$$\omega(r) = \omega_{max} e^{-(r/r_0)^2}.$$

It is easy to see that the total circulation of such distribution is

$$\gamma = \pi \omega_{max} r_0^2. \tag{I.1}$$

The circulation is estimated using this formula, while ω_{max} is measured directly, and r_0 is defined by $\omega(r_0)/\omega_{max} = e^{-1}$.

A.1. Homogeneous isotropic turbulence

We use data in (Ruetsch & Maxey, 1991). Their cores are described as having a mean diameter of 6η at an enstrophy level $9.5 < \omega_i^2 >$, while the maximum recorded enstrophy is given as $80 < \omega_i^2 >$. Their mean diameter can then be used directly to estimate r_0, resulting in an approximate circulation for their cores of $\gamma/\nu \simeq 250$. The aspect ratio of their vortices is given in the paper as $L/D \simeq 6$.

A.2. Wall region of turbulent channels

Kim, Moin & Moser (1987), in their analysis of their numerical simulations of channel flow at $Re_\tau = 180$, introduce a "typical longitudinal eddy" whose vorticity and diameter satisfy

$$\omega_x \nu / u_\tau^2 \simeq 0.13, \qquad u_\tau D/\nu \simeq 30. \tag{I.2}$$

They derive these parameters from the behavior of the ω'_x near the wall. The resulting circulation is

$$\gamma/\nu = (\omega_x/\nu)(\pi D^2/4) \simeq 90$$

Robinson (1989), using the same data set, publishes histograms of vortex diameters and circulations. The mode and average value for the former are $u_\tau D/\nu \simeq 25$ and 35, while for the latter they are $\gamma/\nu \simeq 60$ and 160. Both analyses are in rough agreement.

The values in (I.2) can be interpreted in a slightly more fundamental way. It is usually accepted that the velocity scale in the wall region is the friction velocity, $u_\tau = (\nu \partial u_1/\partial y)^{1/2}_{wall}$ (Tennekes & Lumley, 1972, ch. 5), and that the fundamental structure in that region is a longitudinal velocity streak, whose width, W, satisfies $u_\tau W/\nu \simeq 100$ over a wide range of Reynolds numbers. It has also been shown (Jiménez & Moin, 1991), that each streak contains a single streamwise vortex, and that the presence of the vortex is enough to generate most of the phenomena associated with the streak (Orlandi & Jiménez, 1991). Let us now interpret the second half of (I.2) as $D \simeq W/3$. The first part can then be written in terms of the velocity, v_r, induced by the vortex at its periphery, as

$$v_r = \omega_x D/4 \simeq u_\tau. \qquad (I.3)$$

Such a simple relation raises the hope that the scalings in (I.2) hold independently of Reynolds number, but a careful analysis of data both from minimal channels at different Re_τ (Jiménez & Moin, 1991), and from the full size channel in (Kim, Moin & Moser, 1987) show that, while the diameter of the strongest vortices scales reasonably well in wall units as $u_\tau D/\nu \simeq 20$, their peak vorticity and total circulation increase almost linearly with Reynolds number, from $\gamma/\nu \approx 130$ $Re_\tau = 100$, to $\gamma/\nu \approx 270$ at $Re_\tau = 200$ (Fig. 3). Note that the large error bars in the figure are due as much to real statistical scatter in the data as to arbitrariness in the definition of what really constitutes a vortex. This arbitrariness also explains in part the difference between our values for the full channel data and those of Robinson (1989). The criteria used here among different Reynolds numbers were, however, held consistent and the trend is reliable.

A similar dependence of the near wall variables on the bulk Reynolds number was documented in (Wei & Willmarth, 1989), where it was attributed to differences in the stretching of the structures of the wall region by the outer flow.

The statistics for r.m.s. vorticity near the wall are at present only available for the (Kim, Moin & Moser, 1987) channel. In that case, $\omega_{max}/\omega' \approx 4.6$.

A.3. Homogeneous shear flow

We use data from (Rogers & Moin, 1987). That paper contains a numerical simulation of a turbulent flow in a homogeneous shear, S, developing in time from $Re_\lambda = 81$, at $t = 12$, to $Re_\lambda = 97$ at $t = 18$. Strong vortices appear as hairpins, whose legs are initially aligned approximately with the direction of maximum average strain. Later they rotate to become more nearly streamwise and seem to reach some sort of equilibrium. A possible estimate for the vortex diameter is the first zero crossing of the vorticity autocorrelation function with respect to separations normal to the plane defined by the hairpins, which results in $D(S/\nu)^{1/2} \simeq 2.8$. A visual inspection of the flow fields suggest a value closer to $D(S/\nu)^{1/2} \simeq 5.8$, which does not seem to change much as time progresses. This later value, however, is close to three numerical mesh spacings, and should be used with care. As maximum vorticity we have used twice the author's estimate of three times the r.m.s. vorticity of the flow. This was checked by visual inspection of the flow field at two

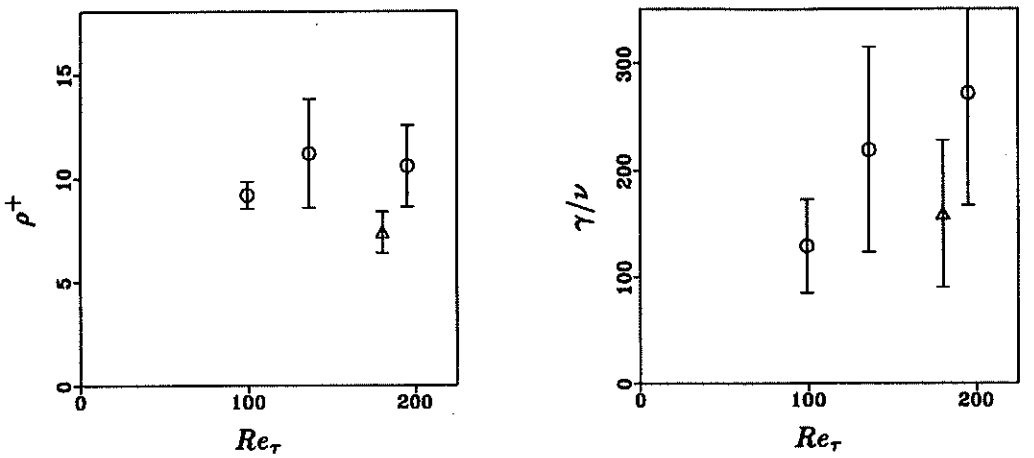

FIGURE A. 1. Radius and circulation of strong streamwise of vortices in the near wall region. Expressed in wall units.

different times in the evolution of the flow. As the turbulence becomes stronger, the maximum vorticity increases from $\omega/S \approx 15$ to 19, but the ratio of ω_{max} to the r.m.s. vorticity stay roughly constant (~ 5.6). The resulting circulation varies from $\gamma/\nu \approx 400$ to 500.

It should be emphasized that the whole simulation corresponds to a developing stage of the flow and that the peak vorticity increases continuously, while the width of the autocorrelation function does not show signs of decreasing. It appears that the hairpins grow in intensity by accreting new vortex lines, rather than just by stretching the existing ones.

A.4. Plane mixing layer

The data are taken from the numerical simulation of a plane, three dimensional shear layer by Moser & Rogers (1991), and from some later simulations by the same authors. Two fields are analyzed, one right before the second pairing ($t = 40$), and another one right after it ($t = 48$). Both fields look visually turbulent, although the outlines of the large spanwise vortex rollers are still apparent. Tubular vortices are visible and, in the edges of the two dimensional rollers, seem to be associated to the rib vortices that dominate the braid region at an earlier stage of the flow, especially in the first field. In the center of the rollers, and in most of the second field, this association cannot be made with any certainty. A characteristic vortex diameter in both cases is $D/\delta_{\omega 0} \simeq 0.20$, where $\delta_{\omega 0}$ is the initial vorticity thickness of the layer. The peak vorticity of the cores is $\omega \delta_{\omega 0}/\Delta U \simeq 5.4$ in the second field, and slightly higher in the first one, but that difference decreases when one particularly strong rib vortex pair is separated from the sample. The total circulation per core is $\gamma/\nu \simeq 340$.

The r.m.s. vorticity at the center of the layer is $\omega' \delta_{\omega 0}/\Delta U \simeq 0.27$, so that $\omega_{max}/\omega' \approx 20$. This value is larger than in any of the other flows, which can probably be explained by the large persistent strain induced by the two dimensional spanwise rollers, as well as by the artificially lowered value of the r.m.s. due to large

scale intermittency.

In the first field, the vorticity thickness of the layer is $\delta_\omega = 8.5$, while in the second it has grown to 10.0. Since the velocity difference across the layer is always $\Delta U = 2$, the peak vorticities of the cores are almost twenty five times larger than the average shear across the layer $\Delta U/\delta_\omega$, but do not seem to scale directly with it.

Appendix II: Principal strains of a Burger's vortex

The vorticity distribution for an equilibrium Burgers' vortex, whose circulation is νRe_γ, subject to an extensional axial rate of strain $w = \alpha z$, is (Batchelor, 1967)

$$\omega(r) = \frac{\alpha Re_\gamma}{4\pi} e^{-\alpha r^2/4\nu},$$

where r is the radial coordinate, and the vorticity vector is directed along the z axis. The corresponding rate of strain tensor has three eigenvalues. The first one is $\sigma_0 = \alpha$, and its eigenvector is aligned with z. It corresponds to the driving strain. The other two are

$$\sigma_\pm = \alpha \left(-\frac{1}{2} \pm \frac{Re_\gamma}{8\pi} F(r/r_0) \right),$$

where $r_0 = 2(\nu/\alpha)^{1/2}$ is the $1/e$ radius of the vortex and

$$F(\zeta) = \frac{1 - (\zeta^2 + 1)e^{-\zeta^2}}{\zeta^2}.$$

One of these eigenvalues is extensional, while the other is compressional, and their eigenvectors are in the equatorial plane, oriented roughly $\pm 45^0$ away from the radial direction. Their magnitude with respect to the driving strain can be characterized by the ratio

$$\frac{\sigma_+ - \sigma_-}{2\sigma_0} = \frac{Re_\gamma}{8\pi} F(r/r_0).$$

This quantity vanishes both at the center of the vortex and at infinity, where the driving strain prevails, but has a maximum at $r/r_0 \approx 1.339$, where

$$\left(\frac{\sigma_+ - \sigma_-}{2\sigma_0} \right)_{max} \approx .012 Re_\gamma.$$

Since this annular region is also where the energy dissipation,

$$\epsilon = \frac{\nu}{2}(\sigma_0^2 + \sigma_+^2 + \sigma_-^2) = \nu \left(\frac{3\alpha^2}{4} + \frac{Re_\gamma^2 F^2}{32\pi^2} \right),$$

is maximum, this is the ratio that should be compared with the experimental results.